On the seasonal response of intermediate and deep water to surface forcing in the Mediterranean Sea

Mediterranean
Circulation
Atmospheric forcing
Convection
Modelling

Méditerranée
Circulation
Forçage atmosphérique
Convection
Modélisation

Emil V. STANEV [a b], **Hans J. FRIEDRICH** [b], **Stojan V. BOTEV** [c]

[a] Faculty of Physics, Sofia University, 5, Anton Ivanov blvd., bg 1126, Sofia, Bulgaria.

[b] Institute of Oceanography, University of Hamburg, Troplowitzstrasse 7, 2000 Hamburg 54, RFA.

[c] Institute of Oceanology, Academy of Sciences, PO Box n° 152, Varna, Bulgaria.

Received 23/3/87, in revised form 2/12/88, accepted 6/12/88.

ABSTRACT

Numerical experiments were carried out to demonstrate the significance of seasonal forcing for the maintenance of the large-scale circulation in the Mediterranean Sea. The Princeton OGCM was used with seven layers and with resolutions of 1.0 and 0.5 degrees in zonal and in meridional directions, respectively. The large-scale features of bottom topography and of climatological driving functions at the sea surface were prescribed according to real data for depth, salinity, temperature and wind stress.The seasonal experiment was initialized with the model results obtained by forcing the model with annual mean surface boundary conditions. The discussion focuses on the effects of seasonal forcing at the sea surface on the establishment of deep and intermediate water due to winter cooling.

Oceanologica Acta, 1989, **11**, 2, 141-149.

RÉSUMÉ

Réponse saisonnière des eaux intermédiaire et profonde au forçage superficiel en Méditerranée

Des expériences numériques ont été effectuées en vue d'expliquer le rôle du forçage saisonnier dans la circulation à l'échelle de la Mer Méditerranée. Le modèle Princeton OGCM a été utilisé avec sept couches et avec des résolutions zonale et méridienne de 1 à 0,5° respectivement. A l'échelle globale, les caractéristiques de la topographie du fond et les contraintes climatologiques à la surface de la mer ont été fixées en accord avec les données réelles de profondeur, salinité, température et tension du vent.

L'expérience saisonnière a commencé avec les résultats de forçage du modèle par les moyennes annuelles des conditions limites à la surface.

Le forçage superficiel saisonnier est discuté dans ses effets sur la formation des eaux profonde et intermédiaire lors du refroidissement hivernal.

Oceanologica Acta, 1989, **11**, 2, 141-149.

INTRODUCTION

The seasonal cycle of surface driving forces provides an important signal for ocean response, including mean circulation. Some processes connected with the ventilation of the thermocline, *e.g.* intermediate and deep water formation, depend strongly on the seasonality. The response of a coupled atmosphere-ocean-ice model to the seasonal variation of insolation has been studied by Wetherald and Manabe (1972). The ocean part of their model was basically the same as the ocean model studied here. Wetherald and Manabe found an unrealistic weakening of the meridional circulation for the case of seasonal forcing as compared to annual mean forcing. This was the consequence of an overestimation by the model of the retreat of the snow/ice cover during summer associated with a reduced meridional temperature contrast.

0399-1784/89/02 141 9/$ 2.90/© Gauthier-Villars

This unexpected and unrealistic result exemplifies the difficulty of estimating in advance the response of a system to seasonal forcing. The results depend on the model physics and in particular on the nonlinearities in the governing equations. Wetherald's and Manabe's 3-component system proved to be extremely sensitive to the albedo feedback mechanism. Similar problems exist in a 1-component system, and numerical experiments with an ocean-only model may contribute to the understanding of specific sensitivities in the ocean response to seasonal forcing.

During the various seasons, convection events produce an asymmetric response of the water column during the heating and the cooling cycles, respectively. This asymmetry makes it necessary to account for these processes at their extreme rates; otherwise, an ocean model cannot be expected to produce an adequate response of intermediate and deep layers. Annual mean forcing underestimates the convective activity.

Convection is a small-scale process, and it necessarily requires subgrid scale parameterization in ocean circulation models. The most simple parameterization involves given surface data of salinity and temperature as functions of time and space, and some kind of adjustment to account for the static stability of the underlying water column. Heat and salt are conserved in the adjustment.

Convection, in particular, is a short time process and is not resolved explicitly with seasonal mean forcing. We expect, however, to find at least in principle the consequences of the asymmetry mentioned above from a comparison between two numerical experiments, one obtained with seasonal forcing and the other with annual mean forcing.

Two different effects are expected: firstly, a quasi-stationary state should evolve more rapidly in those layers ventilated by convection due to its short time scale in comparison with (turbulent) diffusion. This accelerating effect of convective adjustment for the spinup process has already been noticed by Wetherald and Manabe (1972). In their one-dimensional test model of the ocean response forced at the surface by a seasonal heating and cooling cycle, several thousand years of model time were necessary to reach an equilibrium stratification of the water column without adjustment, whereas such a quasi-stationary state was already reached after integrating for two hundred years when convective adjustment was included. The effect can also be seen in the deep-layer temperature trends for the experiments of Manabe *et al.* (1979), who switched from annual mean to seasonal forcing after a certain evolution of their coupled atmosphere-ice-ocean model.

Secondly, the annual mean fields obtained with seasonal forcing should differ from the fields obtained with annual mean forcing. Since it is extremely difficult to anticipate specifications of this difference, numerical experiments with the nonlinear equations controlling the system offer a reasonable approach to investigate this problem.

In order to facilitate validation with observations, it seems appropriate to choose for such an experiment a model of a realistic ocean area, even though irregular forcing and geometry may obscure the model results. Finally, it is reasonable to model an ocean basin of manageable size, where the prevailing surface conditions provide a strong seasonal signal.

In this respect, the Mediterranean Sea can be regarded as an excellent natural laboratory. Here, the total range of sea surface temperature covers approximately 6°C in the annual mean as well as in the winter and in the summer data. Locally, however, the annual range may be twice as large, *i.e.* ~12°C.

Physical processes in the Mediterranean Sea have stimulated the interest of marine scientists for many decades. Recent surveys of the accumulated knowledge are given by Anati (1977), Béthoux (1979), Ovchinnikov (1976), Lacombe (1984) and others. At present, comprehensive international research programmes are being carried out to investigate specific aspects in great detail, including modelling activities (*e.g.* UNESCO, 1985).

For these reasons, we chose the Mediterranean Sea as a test area for our experiments. The present paper includes the following sections: description of the model; model forcing; discussion of model results; summary and conclusions.

DESCRIPTION OF THE MODEL

Bryan's (1969) general circulation model and Semtner's (1974) Fortran code have been used in this study. These references give details of the physics, the solution method and the finite difference scheme. In spherical coordinates (λ, φ), with the vertical (z) pointing upwards and in standard notation, the governing system of equations is:

$$u_t + \Gamma(u) - fv = -ma^{-1}(p/\rho_0)_\lambda + F^u \quad (1)$$

$$v_t + \Gamma(v) + fu = -a^{-1}(p/\rho_0)_\varphi + F^v \quad (2)$$

$$g\rho = -p_z \quad (3)$$

$$\Gamma(1) = 0 \quad (4)$$

$$(S, T)_t + \Gamma(S, T) = F^{S,T} \quad (5)$$

$$\rho = \rho(S, T, p) \quad (6)$$

The momentum equations (1)-(3) have been simplified by the Boussinesq and hydrostatic approximations. Γ is an advection operator for any scalar quantity μ:

$$\Gamma(\mu) = ma^{-1}[(u\mu)_\lambda + (v\mu m^{-1})_\varphi] + (w\mu)_z \quad (7)$$

Thus, (4) is the continuity equation. The effects of turbulent mixing are parameterized by the divergence of an anisotropic stress tensor:

$$F^u = A_{MV} u_{zz} + A_{MH} a^{-2} [\nabla^2 u + (1 - m^2 n^2) u - 2nm^2 v_\lambda] \quad (8)$$

$$F^v = A_{MV} v_{zz} + A_{MH} a^{-2} [\nabla^2 v + (1 - m^2 n^2) v + 2nm^2 u_\lambda] \quad (9)$$

∇ gives the horizontal part of the gradient operator.

The corresponding Laplacian of a scalar μ is:

$$\nabla^2(\mu) = m^2 \mu_{\lambda\lambda} + m(\mu_\varphi / m)_\varphi \tag{10}$$

Turbulent mixing in the conservation equation (5) for salt and heat parameterizes convection effects by instantaneous adjustment. With μ now for either salinity S or for temperature T:

$$F^\mu = [(A_{\mu v}/\delta)\mu_z]_z + A_{\mu H} a^{-2} \nabla^2 \mu \tag{11}$$

$$\delta = \begin{cases} 1 & \text{for } \rho_z \leqq 0 \\ 0 & \text{for } \rho_z > 0 \end{cases} \tag{12}$$

Density ρ is computed from the equation of state (6) using Eckart's (1958) empirical rational. In the above equations, $m = \sec\varphi$ and $n = \sin\varphi$; $f = 2\Omega n$ is the Coriolis parameter. Radius a, gravitational acceleration g and rotation rate Ω of the Earth are taken to be constants. The vertical and horizontal turbulent mixing coefficients, $A_{\mu V}$ and $A_{\mu H}$, for momentum ($\mu = M$) and for tracers ($\mu = S, T$) are also assumed to be constants. Besides S, T, the pressure p and the velocity components (u, v, w) in λ-, φ- and z-directions are the unknown variables. The system of equations is closed with boundary conditions at the sea surface, $z = 0$, at the bottom, $z = -H(\lambda, \varphi)$, and at the lateral boundaries (normal to $\underline{n}$):

At $z = 0$

$$\begin{gathered} \rho_0 A_{MV}(u_z, v_z) = (\tau^\lambda, \tau^\varphi) \\ w = 0 \\ \text{(rigid lid)} \\ (S, T) = (S^0, T^0) \end{gathered} \tag{13}$$

At $z = -H$

$$\begin{gathered} u_z = v_z = 0 \\ \text{(no bottom friction)} \\ w = -(mu H_\lambda + v H_\varphi)/a \\ (S_z, T_z) = 0 \\ \text{(no normal flux)} \end{gathered} \tag{14}$$

At lateral boundaries

$$\begin{gathered} u = v = 0 \\ \text{(no slip)} \\ (\underline{n}\nabla S, \underline{n}\nabla T) = 0 \\ \text{(no normal flux)} \end{gathered} \tag{15}$$

The symbols used in the model equations are standard; τ^λ and τ^φ are the zonal and the meridional components of wind stress at the sea surface; S^0 and T^0 are salinity and temperature of the top layer of the model. These forcing functions will be described in the next section. The bottom relief H is resolved approximately by using different numbers of computational levels at different locations. Computational levels are fixed at 25, 100, 200, 350, 1,000, 2,000 and 3,000 m. The grid steps are $\Delta\lambda = 1°$ and $\Delta\varphi = 0.5°$, in zonal and meridional directions, respectively, to account approximately for the convergence of meridians. The same constant value ($A_{\mu H} = 10^7\,\text{cm}^2\,\text{s}^{-1}$) is used for the horizontal exchange coefficients of momentum and tracers. The vertical exchange coefficients are $10\,\text{cm}^2\,\text{s}^{-1}$ for momentum and $1\,\text{cm}^2\,\text{s}^{-1}$ for the tracers.

The configuration of the model domain is shown in Figure 1.

The figure includes the nomenclature for the various sub-basins mentioned in the text below. It further includes the positions of four sections to be discussed in the text. The main islands of the Mediterranean are resolved by the model. The coarse vertical and horizontal grid spacing cannot, however, adequately resolve many features of the complex bottom relief, which are expected to strongly influence the circulation. Nor, of course, does this model resolve the important physical scale of the Rossby deformation radius necessary for the simulation of mesoscale processes. Finally, the model domain was treated as a completely closed basin. In particular, the Strait of Gibraltar with its important exchange flows between the Atlantic Ocean and the Mediterranean Sea is kept closed in the numerical experiments. In view of these severe restrictions, the model results should be interpreted with great caution.

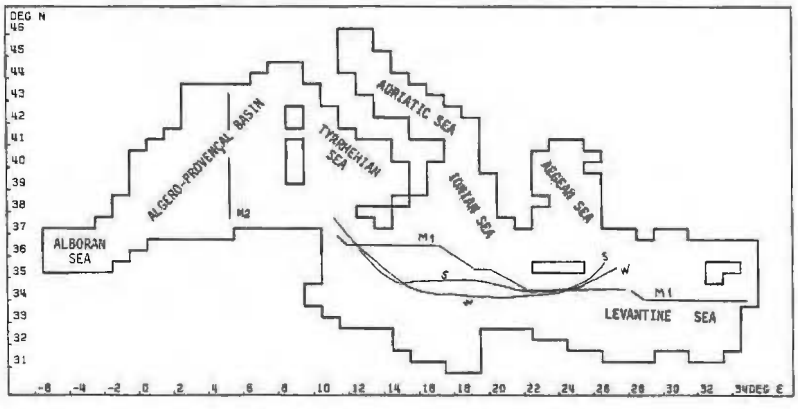

Figure 1
Configuration of the model for the Mediterranean Sea. M1 and M2: positions of model sections used in Figures 5, 6, and 9; S and W: positions of Wüst's (1960) summer and winter sections respectively.

CLIMATOLOGY OF OBSERVATIONS AND OF MODEL FORCING

At the sea surface of our model, Dirichlet boundary conditions for temperature and salinity are used as driving forces together with the momentum flux by wind stress. These surface boundary data are taken from observations and a few comments are given concerning their space and time characteristics. Four seasonal fields are used by the model with linear interpolation between them to describe the time variation.

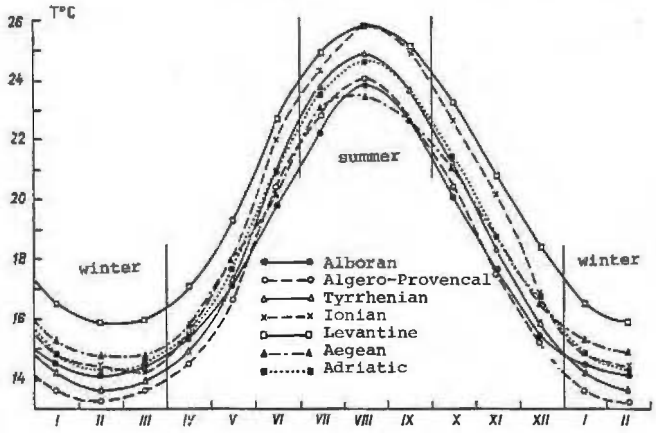

Figure 2
Observed seasonal cycles of sea surface temperature in selected areas of the Mediterranean Sea (Ovchinnikov et al., 1976).

The phase of all driving functions in (13) is chosen to correspond to Becker's (1978) salinity seasons. Thus, the model summer is centered on August, the month of maximum surface temperatures (*see* Fig. 2).

Wind stress was computed from seasonal pressure data (Ovchinnikov, 1976) using Ekman boundary layer approximation. Generally cyclonic throughout the year, the wind field intensifies in winter, especially in certain locations along the northern coast where the airflow is channelled by the particularities in topography and in the land-sea distribution. In summer, easterly winds are observed close to the African coast in the Western basin, changing the sense of rotation. These main characteristics are incorporated in the forcing of the model. Starting with winter, area-averaged magnitudes of the model wind stress are: 0.019, 0.013, 0.015 and 0.014 Pa.

Sea surface data are applied as representative values for salinities and temperatures of the top layer (25 m) in the model. Annual mean distributions of these data are shown in Figure 3. The seasonal and annual mean top layer temperatures for the numerical experiments were computed from Becker's (1980) monthly mean values. Generally, the surface temperature decreases from south to north. Minimum values are observed in the Gulf of Lions, in the Adriatic and in the Aegean Sea. This general pattern is qualitatively the same in all seasons. The seasonal change in surface temperature is close to sinusoidal with minimum values in February and maximum values in August. The amplitude is approximately 12°C in all basins (compare Fig. 2).

Seasonal surface salinity data are taken from Becker's (1978) maps. The inflow of Atlantic water specifies the minimum (37.00) of the overall pattern. Strong local minima are due to the inflow of Black Sea water in the northern Aegean Sea (35.00), and due to river discharge in the northern Adriatic Sea (36.00). The maximum surface salinity is found in the Levantine Sea (39.25). In particular the local minima are subject to strong seasonal changes (induced by changes in the diluting sources). Compared with temperature, seasonal changes in surface salinity are less regular in time and space. A few general features, however, are noteworthy:

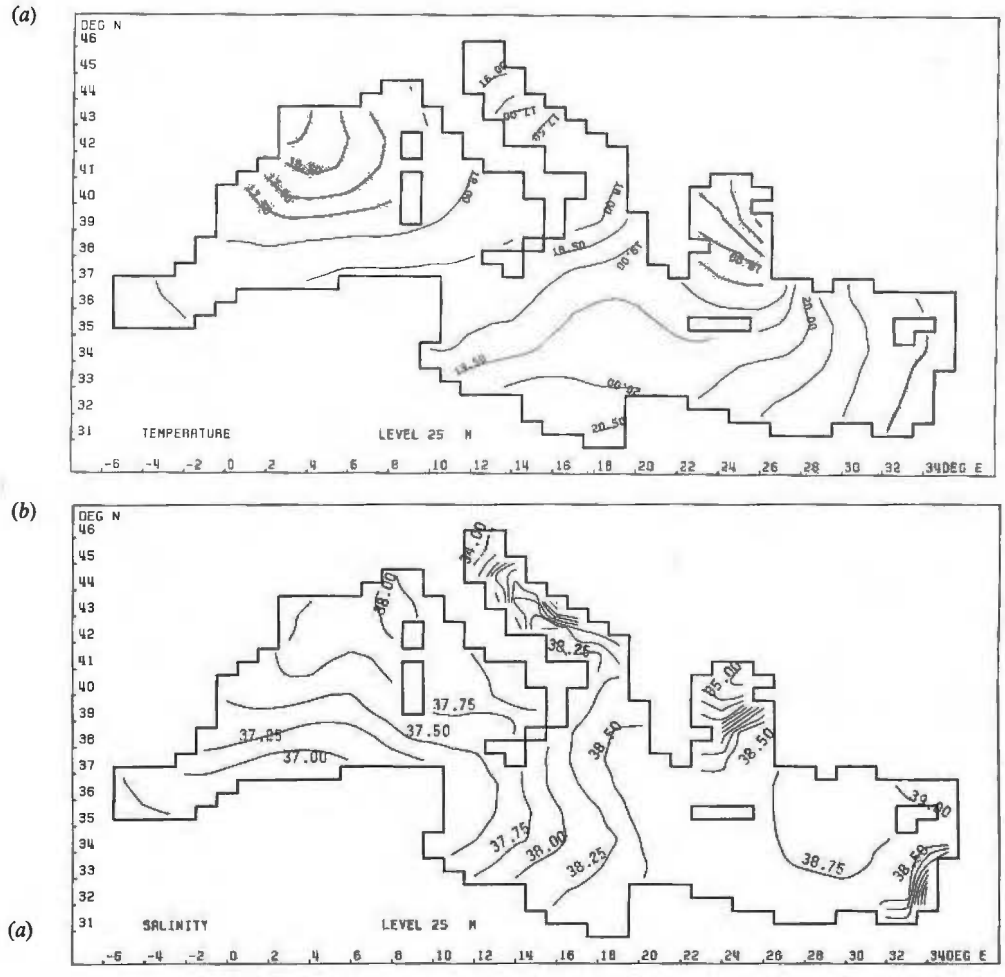

Figure 3
Annual mean values of temperature (a) and salinity (b) at the sea surface.

in the Eastern basin, surface salinity has maximum values of 39.25 during summer and fall. During winter and spring, the surface salinity here lies in the range 38.75-39.00. The opposite phase is generally observed in the Western basin. Affected by seasonal changes in the balances at the Gibraltar strait the surface salinity off the African coast also decreases, however, from summer to winter by about 0.25. In the intermediate region of the Ionian Sea, amplitudes of the seasonal change in surface salinity are small. More phase shifts with respect to the central Eastern basin are observed towards the Adriatic and Aegean Seas, where local effects give rise to annual amplitudes of several salinity units. A secondary salinity maximum occurs in the Gulf of Lyon. It is anticipated that this high positive salinity anomaly, which is caused by the upwelling of intermediate water in conjunction with strong seasonal winds and surface cooling, controls the deep water formation in the northern part of the Western basin.

Strong variations in the vertical stratification are the consequence of the variability in space and time of surface boundary conditions. The difference between horizontally averaged density at 700 m, ρ 700, and the density ρ_0 at the sea surface is shown in Figure 4 for winter, for summer and for the annual mean data. The 700 m-level is shallow enough not to lose the information of a large coastal area and deep enough to use reference density values from layers below the Levantine water. In summer, the vertical stability increases considerably due to surface heating. This increase is particularly strong along the North African coast. In the northern parts of the Aegean Sea and of the Adriatic Sea the summer increase in stability is due rather to the decrease in sea surface salinity caused by river inflow. Winter cooling destabilizes the vertical structure. This destabilization is most pronounced in the northern part of the Algero-Provençal basin and in the south-eastern part of the Aegean Sea (Fig. 4 *a*). Both areas are sources of deep and intermediate water.

The annual mean pattern of the density difference $\Delta\rho$ is geometrically similar to those in winter and in summer. Relative to the winter season, however, the difference is stronger by factors of 2.4 in the northern Algero-Provençal basin and 1.8-2 in the northern Levantine basin. A model which lacks this winter-time destabilization and also the particularly intense mechanical surface forcing during this season severely restricts the downward penetration of surface water and reduces the ventilation of deep and intermediate layers.

In our model, the strait of Gibraltar is closed, which is a serious limitation. The model circulation cannot be expected to correspond to observations, particularly in the vicinity of the strait and possibly along the North African coast. Some traces of the exchange with the Atlantic Ocean, however, are maintained by prescribing the Atlantic Water with its surface temperature and salinity in the boundary conditions.

DISCUSSION OF MODEL RESULTS

We discuss below the results of two model experiments. In the first, annual mean atmospheric forcing is used.

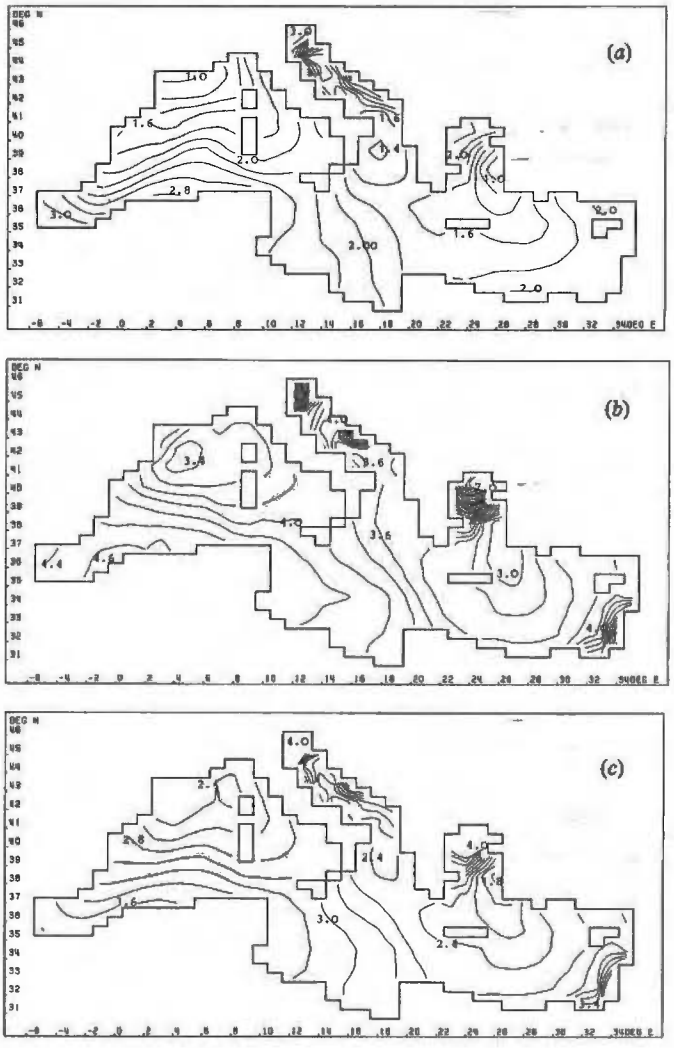

Figure 4

Stability of the water column, as given by the difference between the horizontally averaged density at 700 m and the density at the sea surface: a) winter; b) summer; c) annual mean.

In the second, forcing incorporates the seasonal variability in boundary conditions. The baroclinic signal penetrates from the surface into deeper layers and changes there the distribution of temperature and salinity. The rate of establishment of horizontal gradients in these hydrophysical fields indicates the speed of convergence of the model towards a quasi-equilibrium state. The comparison between results of the two experiments and between model simulations and observational data demonstrates the role of seasonal variability in deep water formation.

Experiment with annual mean forcing

Annual mean surface boundary conditions obtained by averaging seasonal data are used for an initial test of the model evolution towards a quasi-equilibrium state. Integration is started from rest with area averaged annual mean vertical profiles of temperature and salinity.

In the first 3-4 years, the currents in the upper layers adjust to boundary conditions and the kinetic energy of the model circulation rapidly increases. This change then becomes more gradual, and is associated with the deep layer adjustment. The experiment is interrupted

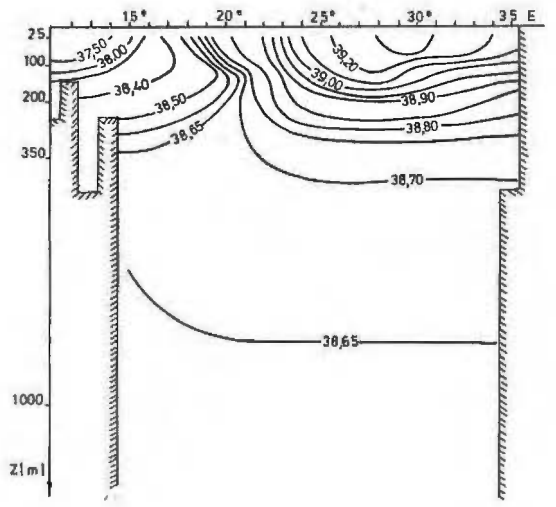

Figure 5
Vertical salinity section along M1 of Figure 1 (annual mean forcing).

after 10 years of integration. This is before a full adjustment has been accomplished. In spite of remaining trends, however, the results provide some insight, and we show some of them anticipating in particular a comparison with the seasonal experiment.

Figure 5 displays the computed salinity cross-section M1 in the Eastern Mediterranean Sea (*see* Fig. 1). Wüst's corresponding summer and winter sections are given in Figures 6*a* and 6*b*. There is some general agreement between the observed and computed sections in the upper 200-300 m. The model results indicate the tendency to form an intermediate layer of Levantine water in the Eastern Mediterranean. The deeper layers, however, have not adjusted to the surface boundary conditions. The deep temperature and salinity patterns are still dominated by the horizontal homogeneity of the initial conditions. The range of computed temperature at 100 m covers only 2°C. This is less than half the observed temperature range—Ovchinnikov *et al.* (1976).

The horizontal distribution of salinity at 100 m is shown in Figure 7. At this level, the distribution is quite similar to that at the sea surface given in Figure 3*b*. The diffusive vertical transport of salt smoothly penetrates the intermediate layers. In the central part of the sea, where Atlantic and Levantine waters meet, the isohalines have north-south directions. The salinity maximum is obtained between Cyprus and Crete. The dilution induced by surface boundary conditions in the Aegean Sea, in the Adriatic Sea and at the Strait of Gibraltar is still noticeable at 100 m. At this early stage of integration the horizontal salinity gradients decrease strongly below 300 m. At 1000 m, for instance, the maximal salinity contrast does not exceed 0.02, which is more than one order of magnitude less than the observed contrast (Ovchinnikov *et al.*, 1976).

There are two obvious reasons for this discrepancy between the results simulated after 10 years of integration and the observational data. First, the time of integration is, of course, insufficient for an adjustment of the prognostic fields in deep layers to the surface forcing. The surface signal penetrates downwards with the vertical diffusion time scale, and it requires integra-

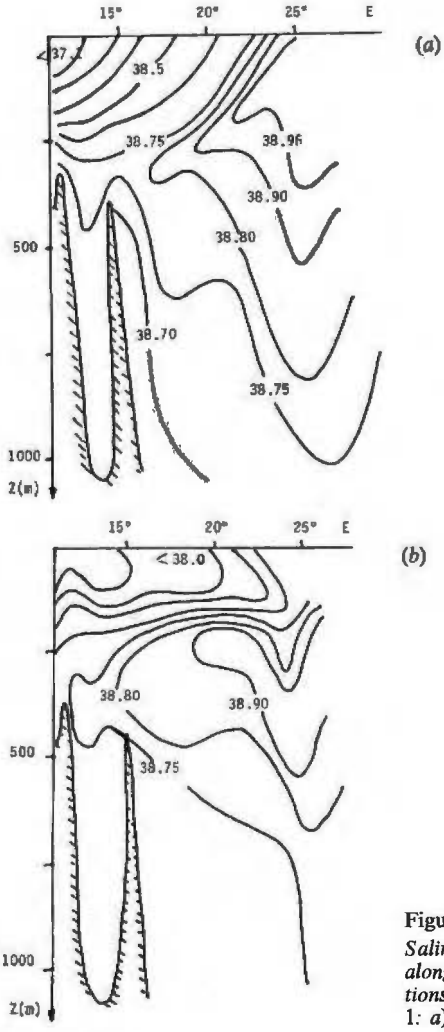

Figure 6
Salinity distributions along Wüst's (1960) sections W and S of Figure 1: a) winter; b) summer.

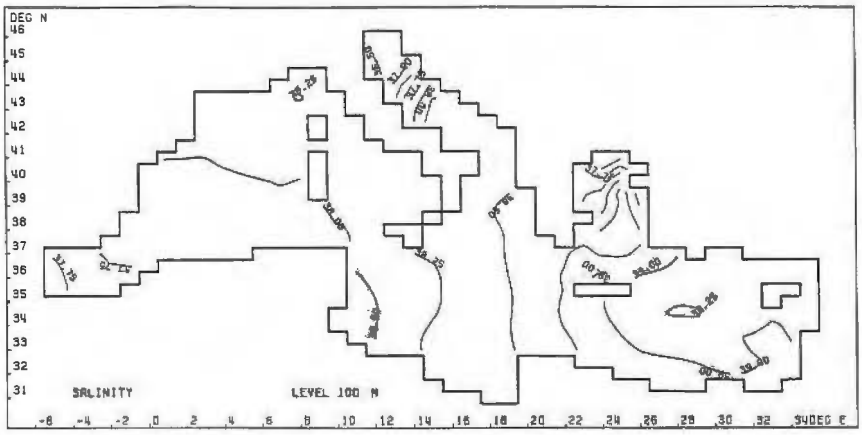

Figure 7
Salinity at 100 m (annual and mean forcing).

tion times of the order of several hundred or thousand years to reach quasi-stationary equilibrium in the stratification of the full water column. The second reason may be the neglect of the time variability in sea surface boundary conditions which could be crucial for the deep layer adjustment. The numerical integration of the model after this stage was therefore continued with seasonal forcing at the sea surface.

Response of the model to seasonal forcing

With seasonal forcing applied, the model results obtained after 10 years with annual mean forcing change rapidly and drastically. It should be noted that the diffusion time scale does not control the spin-up time, if convective processes during the cooling season play a dominant role. In terms of total kinetic energy, a quasi-periodic state is already reached after four years of integration.

The seasonal change of kinetic energy averaged over the total volume is shown in Figure 8. Its annual mean value is approximately 50% higher than the kinetic energy in the first stage of integration with annual mean boundary conditions. This increased energy level is a direct consequence of the annual variability in the forcing and of the nonlinearity of the system. The energy maximum occurs in winter (January and February). This corresponds to intense wind forcing during this season. During summer and autumn, the changes in energy are comparatively small.

The seasonal variations of the model circulation penetrate down to the deep layers. The continual change of the atmospheric forcing leads to strong local convection and to the establishment of correspondingly strong horizontal gradients in temperature and salinity of the deep layers. While in the first experiment with annual mean forcing, the salinity range at 1 000 m was only 0.02, in the experiment driven by seasonal forcing this range has increased to 0.12 after only four years of integration. This computed range is very close to the observed one.

The effectiveness of seasonal forcing for the penetration of the buoyancy signal into intermediate and deep layers can be observed on the vertical cross-sections for the summer and winter seasons. The sections

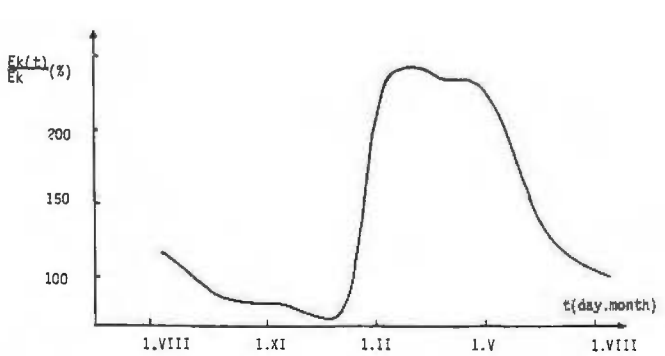

Figure 8

Seasonal variation of the kinetic energy averaged over the total volume of the sea (%). The kinetic energy for the numerical experiment with stationary atmospheric forcing (Ek) is taken as 100%.

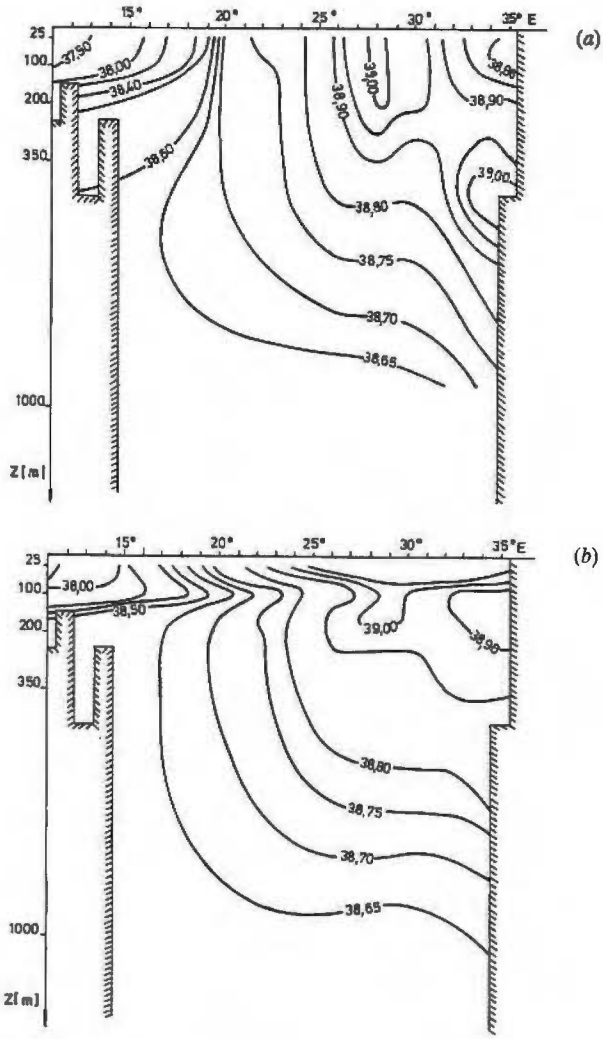

Figure 9

Vertical salinity cross-sections along M1 of Figure 1 (seasonally variable forcing); a) winter; b) summer.

displayed in Figure 9 correspond to the section of Figure 5, but in the case of seasonal forcing the agreement with Wüst's (1960) observed sections displayed in Figures 6*a* and 6*b* has improved considerably. This obviously indicates the trend of the model to simulate the formation of Levantine water in the northern part of the Levantine basin. The currents (Fig. 10) simulated by the model give a generally westward flow for the intermediate layers with a speed of about 0.01 m/s. This westward flow can also be inferred from the shape of isohalines in Figure 9. The numerical model simulates the subsurface salinity minimum in the central basin. This minimum exists only in summer, the time of strongest evaporation, and vanishes in winter (compare also with the Wüst (1960) summer section, Fig. 6*b*).

The salinity values simulated by the model in the North Liguro-Provençal basin are higher than the values in the rest of the Western basin. This is in agreement with the observations documented by Ovchinnikov *et al.* (1976), and others. The model also simulates strong upwelling in this area during winter, and the isohaline surfaces rise close to the sea surface. A detailed examination of the salinity distribution indicates that in the North Liguro-Provençal basin the vertical salinity gradient is small. This is an important precondition

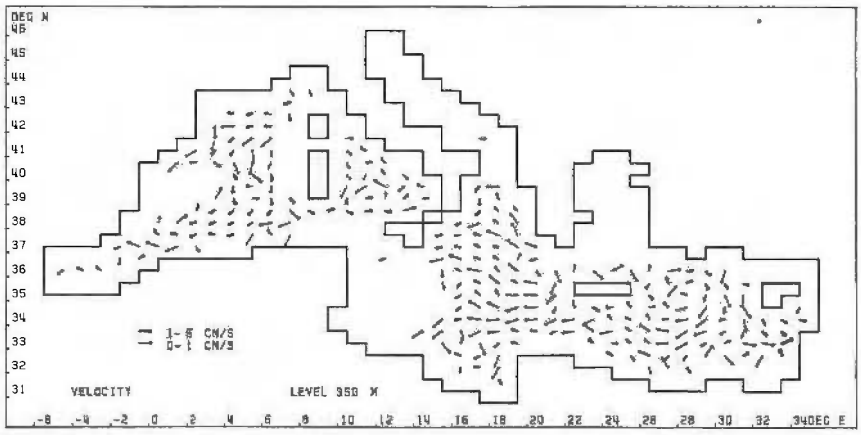

Figure 10
Currents at 350 m in autumn.

for the development of deep convection during winter cooling.

Vertical salinity sections from north to south along M2 (*see* Fig. 1) are shown in Figure 11. The northern part of these sections coincides with the area of strong winter cooling in the vicinity of the Gulf of Lions. As can be seen from Becker's (1978) results sea surface salinity values increase considerably during the winter season. As a result of the decrease in temperature, of the increase in salinity, and of the strong winds the model simulates intense convection and the isohalines close to the northern coast of the Liguro-Provençal basin are almost vertical. This wintertime convection penetrates the intermediate layers and contributes to deep water formation. At the southern end of both sections in Figure 9, minimal salinity values mark the core of the North African current, which transports Atlantic water to the east.

The seasonal variation in atmospheric forcing produces substantial changes of the vertical patterns from winter to summer. In the upper 200 m at the northern end of the section, the isohalines become almost horizontal in summer. However, the summer boundary conditions have no significant effect on the salinity distribution in deep layers, because during this season the penetration of the buoyancy signal is controlled by diffusion. The meridional salinity gradient in intermediate layers persists until convection resumes in the following winter season. Thus the model simulates realistically the Gulf of Lions as an important region of deep water formation.

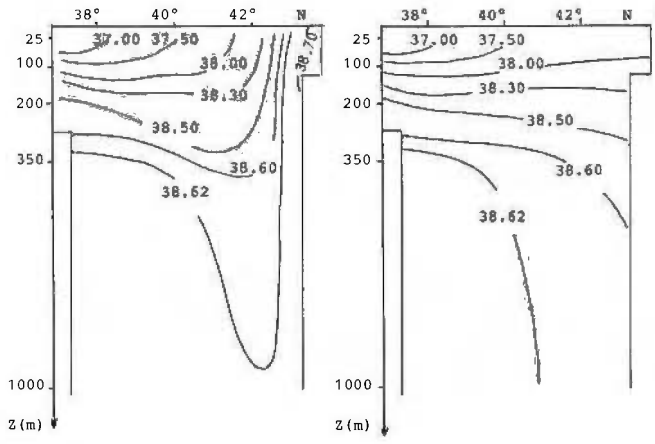

Figure 11
Same as Figure 9 but along M2 of Figure 1.

SUMMARY AND CONCLUSIONS

The main task in the present work was to study the response of the numerical model to seasonal variations in atmospheric forcing. With these variations included, the model converges much more rapidly towards a steady state than in the case of annual mean forcing. If annual mean fields are used as driving functions, the diffusion time scale controls the adjustment of the model to the boundary conditions. Annual mean conditions suppress the convective activity prevailing in winter and then effectively controlling the adjustment of the deep water. The seasonal model results simulate some features of water mass formation which are typical for the Mediterranean Sea. Among these are the formation of Levantine water and its westward spreading, as well as the deep penetration of surface water due to winter cooling in the northern part of the Liguro-Provençal basin.

We have demonstrated that time variations in surface boundary conditions improve the results of the circulation model for the Mediterranean Sea. Further improvements should be obtained with a better resolution, with open boundary conditions at the Strait of Gibraltar, and with appropriate flux conditions for heat and water at the sea surface instead of the Dirichlet conditions for salinity and temperature used in this investigation. Preliminary results with a model containing such improvements will be presented in a separate paper.

Acknowledgements

The authors thank two referees for useful comments. We also acknowledge the help of S. Beddig, S. Rolinski and C. Hollmeier in preparing the manuscript. One of the authors received support from the Alexander von Humboldt Foundation to carry out part of the studies in the Federal Republic of Germany.

REFERENCES

Anati D. A. (1977). Topics on the physics of the Mediterranean Sea. *Ph. D. Thesis, Weizmann Institute of Science, Rehvot, Israel*, 43 pp.

Becker G. A. (1978). Der Oberflächensalzgehalt des Europäischen Mittelmeeres. *Dt. hydrogr. Z.*, **31**, 190-194.

Becker G. A. (1980). Die Temperatur an der Oberfläche des Europäischen Mittelmeeres. *Dt. hydrogr. Z.*, **33**, 255-270.

Bethoux J.-P. (1979). Budgets of the Mediterranean Sea. Their dependence on the local climate and on characteristics of the Atlantic waters. *Oceanologica Acta*, **2**, 2, 137-163.

Bryan K. (1969). A numerical method for the study of the circulation in the World Ocean. *J. comp. Phys.*, **4**, 3, 347-376.

Lacombe H. (1984). General Physical Oceanography of the Mediterranean Sea. In: *Proceedings of the NATO Advanced Research Workshop, La Spezia*, H. Charnock, editor.

Manabe S., K. Bryan and M. J. Spelman (1979). A global ocean-atmosphere climate model with seasonal variation for future studies of climate sensitivity. *Dynam. Atmos. Oceans*, **3**, 393-426.

Ovchinnikov I. M., E. A. Plachin, L. V. Moskalenko, K. V. Neglijad, A. S. Osadichii, A. F. Fedoseev, V. G. Krivosheja and K. V. Voitova (1976). *Hydrology of the Mediterranean Sea*, Leningrad, Gydrometeoizdat, 375 pp. (in Russian).

Pacanowski R. C. and S. G. H. Philander (1981). Parameterization of vertical mixing in numerical models of tropical oceans. *J. phys. Oceanogr.*, **11**, 1443-1451.

Semtner A. J. (1974). An oceanic general circulation model with bottom topography. Numerical simulation of weather and climate, Technical Report N9, University of California, Los Angeles, 99 pp.

Stommel H. (1972). Deep winter-time convection in the western Mediterranean Sea. In: *Studies in Physical oceanography*, vol. 2, A. L. Gordon, editor, Gordon and Breach, New York, 207-218.

UNESCO Report in Marine Sciences, 30 (1984). Physical Oceanography in the Eastern Mediterranean: an overview and research plan. Report of the Workshop held in Lerici, La Spezia, Italy, September 1983, 16 pp.

Wetherald R. T. and S. Manabe (1972). Response of the joint ocean-atmospheric model to the seasonal variation of the solar radiation. *Mon. Weath. Rev.*, **100**, 1, 42-59.

Wüst G. (1960). Die Tiefenzirkulation des Mittelländischen Meeres in den Kernschichten des Zwischen- und des Tiefenwassers, *Dt. hydrogr. Z.*, **13**, 105-131.